Fifth Meeting of the ENFSI Working Group Marks (SPTM), Stavern, Norway, 24–27 May 2005

Model-Based Segmentation of Striation Marks

Dr. Michael Heizmann

Fraunhofer IITB Institut für Informations- und Datenverarbeitung,
D-76131 Karlsruhe, Germany

ABSTRACT

In forensic science, striation marks form a large and important portion of relevant cues. They comprise the groove patterns on the circumferential surface of bullets, where the individual characteristics of the barrel—production marks as well as damages due to usual wear—are concentrated in strictly straight grooves. Moreover, many tools produce groove-shaped marks when used in a dragging movement. To suppress irrelevant regions without grooves and consequently improve an automated comparison system, a segmentation of the actual groove area on the specimen is useful.

In this contribution, an image processing method is presented that uses an illumination series to robustly segment striation patterns from mainly isotropic background areas. The illumination series is obtained with a spot illumination whose azimuth is varied systematically. The strategy is based on the modeled characteristics of local contrast with respect to the azimuth of the illumination: Whereas pronounced maxima of the local contrast can be observed when the striae are illuminated perpendicularly, an isotropic background texture shows less distinct maxima for random azimuth angles. The qualification of the approach is demonstrated on the segmentation of faint tool marks. Experimental results show that the methodology ensures the correct segmentation of such marks.

Keywords: forensic science, striation mark, segmentation, illumination series, oriented patterns, anisotropy analysis, image fusion

1. INTRODUCTION

Striation marks form an important portion of forensic marks. They originate from grinding or dragging motions of a tool. In consequence, the resulting plastic deformation or local removal of material generates three-dimensional grooves on the surface of the specimen. The grooves can be used to draw conclusions on the tool used. This species of marks comprises the particularly interesting striation marks on the circumferential surface of bullets. Moreover, many tools like e. g. screwdrivers, knives or gripper tools produce similar marks, when they are used in an appropriate manner.

To enable an automated processing and evaluation of striation marks, the recorded images of the specimen have to be transformed into signals—i. e. the signatures—that are suitable for computerized comparison. Fig. 1 shows a possible methodology for processing a macroscopic image of a tool mark.

- The first step is the data acquisition, see Fig. 1(a). A light-macroscopic setup based on a standard macroscope with an additional flexible illumination and positioning device has proven to yield satisfactory raw data.[1–3] However, the processing steps including the segmentation stage this contribution focusses on is not limited to microscopic images, but can be applied to any kind of images revealing the groove-like structure of the marks, like e. g. depth-from-focus methods.[4] To preserve such faint structures, the acquisition and fusion of focus series may be useful.[5]

- In the first processing step, suitable preprocessing operators eliminate undesired signal components, see Fig. 1(b). When light-microscopic images are processed, disturbances are removed that result e. g. from locally inhomogeneous illumination intensities or from the interference of the illumination and the locally varying reflectance properties of the specimen.

Further author information: E-mail: heizmann@iitb.fraunhofer.de;
WWW: http://www.iitb.fraunhofer.de, Telephone: +49-721-6091-329; Fax: +49-721-6091-413

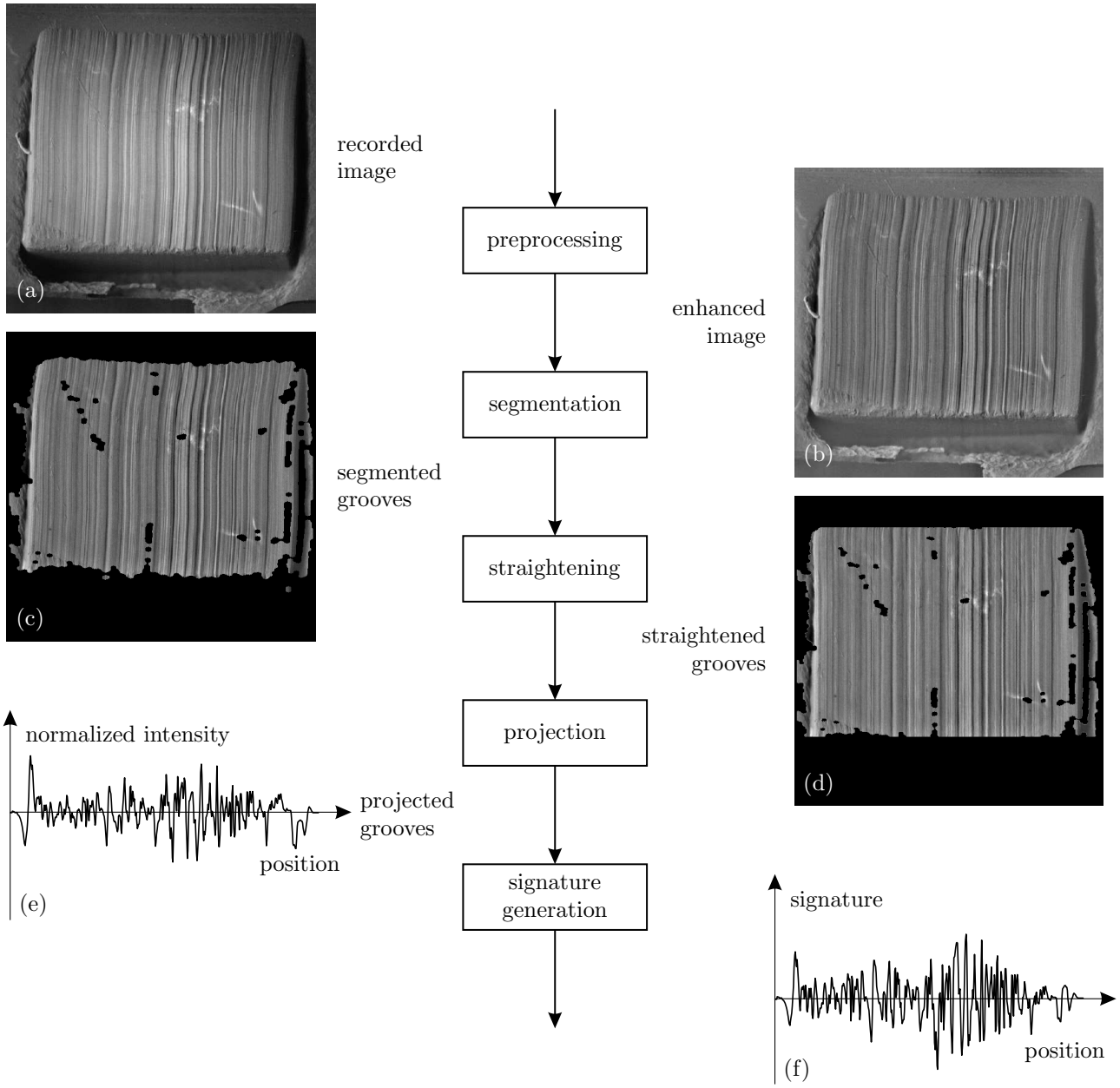

Figure 1. Methodology for processing an image of striation marks. Starting from the recorded image (top right), a meaningful signature (bottom right) is extracted in a multi-stage process.

- At this stage, the actual groove area is segmented, see Fig. 1(c). In the figure, the image parts that do not belong to the groove area are labeled in black. That way, only surface elements that belong to the relevant groove structure are considered in the subsequent evaluation.

- Now, features have to be extracted from the image. A robust feature extraction demands that the entire groove area is processed and included in the resulting signatures. For that purpose, a model-based approach, which takes the kinematics of the groove generation into account, has proven suitable.[1,2,6] The motion parameters of the edge are estimated, leading to a back transformation of the usually curved grooves into straightened grooves, see Fig. 1(d).

- The straightened grooves are then filtered and projected in groove direction, see Fig. 1(e). With this data reduction from two-dimensional images to one-dimensional signals, a more efficient data comparison can be achieved. In addition, the required data storage decreases significantly.

- Since the projections still contain irrelevant disturbances, a postprocessing is appropriate, see Fig. 1(f). In this step, faint but acute peaks are intensified, whereas smoother transitions are attenuated. The result of the overall processing is a signature, which contains the relevant signal part of the striation marks and can be used for an automated comparison.[2,7,8]

By means of a segmentation of tool marks, several favorable effects can be achieved simultaneously:

- Irrelevant areas, which possibly interfere with the identification of marks, are suppressed. Although the projection and filtering in the feature extraction stage equals an attenuation of structures that do not correspond to the marks signal model, undesired signal components are still present. In consequence, the resulting signature would degrade significantly. Figure 2 shows an example of a straightened tool mark. The projection yields a signal consisting of the actual groove profile and artifacts from adjacent areas where no marks are present. In these areas highlighted in gray, only the irrelevant background structure of the specimen contributes to the resulting projection and thus alters the overall signal.

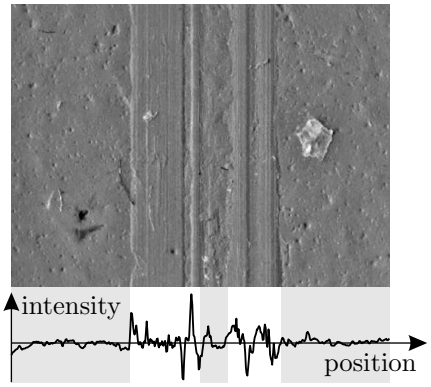

Figure 2. Motivation for the segmentation of striation marks: straightened grooves (above) and projection (below). The grayed parts of the profile represent undesired parts.

- Subsequent processing steps can be optimized to the characteristics of the groove area. Many local filter operations can be accelerated, if they are applied to linear areas instead of two-dimensional areas. In addition, it is sensible to adapt filter masks such that faint groove details in the striation area are emphasized.

- Moreover, the computational expense of the succeeding processing stages often depends on the size of the input signals. Since the segmentation leads to smaller images, the feature extraction takes less computation time. This also applies to the final database search, in which shorter signals reduce the time for the actual comparisons.

2. SEGMENTATION STRATEGY

To design an adequate segmentation methodology for striation marks, previous knowledge on the generation process of the grooves can be deployed. Within the interesting groove texture, the following characteristics are found:

- A unidimensional tool edge has touched the surface of the specimen in a mainly translational motion. The rotation of the tool during this motion is of minor importance and can be neglected.

- If the tool edge is sufficiently structured, the striations are characterized by a strong anisotropy.

- In a small local neighborhood of an image point within the striations, the grooves can be considered as straight. This requires that kinks or sharp bends should not occur.

- Due to shape and translation of the tool edge, overlapping grooves from the same tool do not occur. In cases where overlapping grooves are found from several consecutive treatments, the image processing must be limited to the striations of a single tool, e. g. by masking the striations manually.

In contrast, no specific knowledge is available on the background texture. Its characteristics depend strongly on the manufacturing of the specimen. In practice, spray lacquered, sandblasted or similar surfaces with mainly isotropic texture are often found.

For simplification, it is assumed that the tool has left distinct marks, such that each location can be assigned either to the groove area $\mathcal{T}$ or the background area $\mathcal{B}$, i. e. $\mathcal{T} \cap \mathcal{B} = \varnothing$.

The algorithm that will be explained in the following section generates a binary mask. For the final segmentation, a modified binary mask is used, which has been improved by means of morphological image processing to suppress dot-shaped classification errors.

To test the segmentation techniques presented in this paper, two exemplary marks are processed which represent typical challenges, see Fig. 3: The mark in Fig. 3(a) has well pronounced grooves and must be separated from the background at the strongly visible edge. In contrast, the faint grooves in Fig. 3(b) have gaps, thus requiring the segmentation to dissect several groove areas from the background in a form of patchworking. These exemplary marks are taken from a database consisting of 54 tool marks, which were generated by a forensic institute in order to establish a standard archive for evaluating automated comparison algorithms and systems. The marks were recorded with the image acquisition station described in Refs. 1, 3, which enables a fast and automated image acquisition.

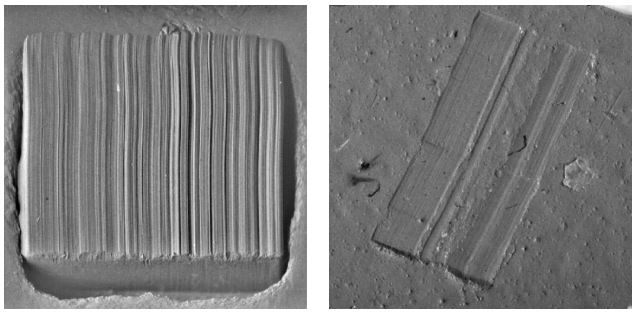

(a) (b)

Figure 3. Test marks for the assessment of the segmentation strategy: (a) distinct grooves; (b) faint grooves with gaps.

3. FUSION OF ILLUMINATION SERIES

To detect the anisotropy of the groove area, the behavior of the local variance (i. e. a measure of the local contrast) is evaluated. The empirical local variance of a neighborhood $\mathcal{N}$ in an image $g(\boldsymbol{x})$ is defined as

$$\operatorname{var}(\boldsymbol{x}) = \frac{1}{|\mathcal{N}| - 1} \sum_{\boldsymbol{\xi} \in \mathcal{N}} \left(g(\boldsymbol{\xi}) - \overline{g}_{\mathcal{N}}(\boldsymbol{x}) \right)^2 , \tag{1}$$

where $\overline{g}_{\mathcal{N}}(\boldsymbol{x})$ denotes the local mean value of the image intensities, and $|\mathcal{N}|$ is the number of pixels in $\mathcal{N}$.

A first approach to use local variance is obtained by considering its dependence on the shape and the orientation of the neighborhood $\mathcal{N}$.[2,9] When $\mathcal{N}$ has a large aspect ratio, i. e. $\mathcal{N}$ is long and narrow, smaller values of the local variance are obtained in case that the longer side is aligned with the grooves as compared to the perpendicular orientation of $\mathcal{N}$. In contrast, when an isotropic background area is processed, the local variance is approximately constant without depending on the orientation of $\mathcal{N}$. This approach can be applied to any single image of a specimen that is recorded with a suitable illumination. However, the segmentation result strongly depends on the illumination direction applied, thus making the segmentation unreliable.

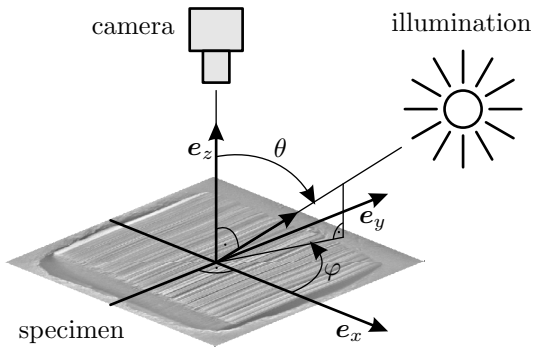

Figure 4. Directions of illumination.

An improved strategy to detect anisotropy is based on image series, in which the azimuth φ of a remote spot illumination is varied systematically, see Fig. 4. The polar angle θ is chosen such that the recorded images have satisfactory contrast. This angle remains constant throughout the series.

When the azimuth φ of the illumination is varied, the local variance shows the following characteristics:

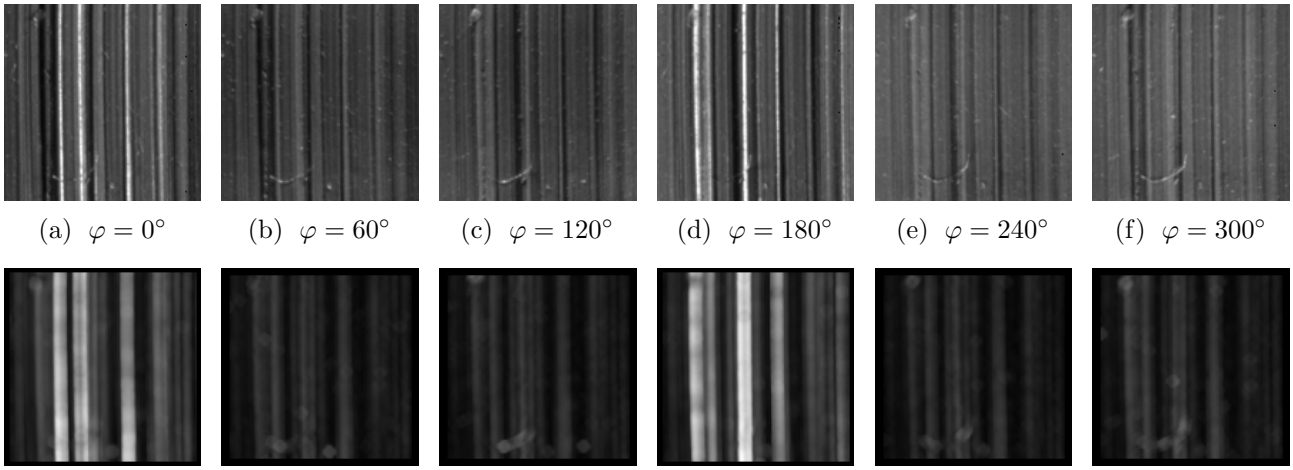

(a) $\varphi = 0°$ (b) $\varphi = 60°$ (c) $\varphi = 120°$ (d) $\varphi = 180°$ (e) $\varphi = 240°$ (f) $\varphi = 300°$

(g) $\varphi = 0°$ (h) $\varphi = 60°$ (i) $\varphi = 120°$ (j) $\varphi = 180°$ (k) $\varphi = 240°$ (l) $\varphi = 300°$

Figure 5. Illumination series of a striation pattern: unprocessed images (upper row); local variance (lower row).

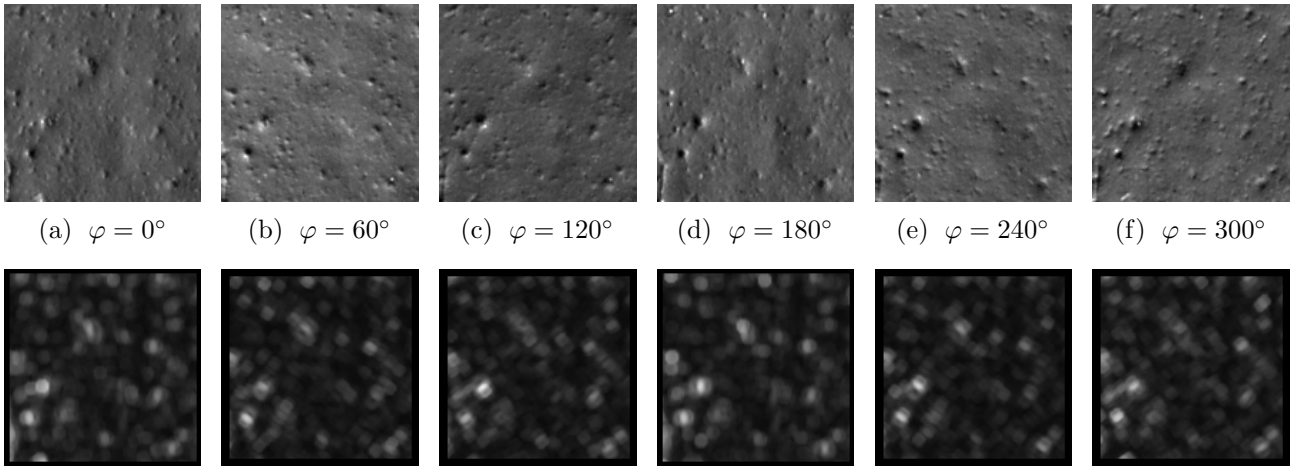

(a) $\varphi = 0°$ (b) $\varphi = 60°$ (c) $\varphi = 120°$ (d) $\varphi = 180°$ (e) $\varphi = 240°$ (f) $\varphi = 300°$

(g) $\varphi = 0°$ (h) $\varphi = 60°$ (i) $\varphi = 120°$ (j) $\varphi = 180°$ (k) $\varphi = 240°$ (l) $\varphi = 300°$

Figure 6. Illumination series of a background texture: unprocessed images (upper row); local variance (lower row).

- Within the groove texture, a maximum of the local variance $\mathrm{var}(\boldsymbol{x}; \varphi)$ can be expected when the illumination is perpendicular to the local groove direction. Thus, the local variance has two maxima for each location $\boldsymbol{x}$. The azimuth angles φ for these maxima are separated by $\Delta\varphi = 180°$.
- In contrast, maxima of the local variance in the background texture occur at random azimuth angles.

The above discussion motivates to employ the local variance as a function of the azimuth as a feature for the segmentation. To accomplish this task, the second harmonic component is evaluated.

Figure 5 illustrates this approach on a striation pattern, which has been illuminated with varying azimuth angles. When the azimuth angle takes the values 0° or 180°, maxima of the local variance can be observed. A typical background texture shows maxima of the local variance at arbitrary azimuth angles, see Fig. 6.

For the implementation of the strategy, further properties of the local variance can be exploited: Within the striation area, large intensity differences should occur in the direction of the illumination, when the illumination

is perpendicular to the grooves, see Figs. 5(a) and (d). In contrast, fluctuations that are oriented perpendicularly to the illumination are attributed to defects in the groove texture and should be suppressed.

3.1. Measurement of the local variance

The computation of a suitable measure for the local variance is done in two stages: Firstly, an anisotropic smoothing suppresses fluctuations which are oriented perpendicularly to the illumination azimuth. In this step, each image of the series is filtered with an individually designed anisotropic Gaussian low-pass filter.[2,9]

Secondly, the local variance $\mathrm{var}(\boldsymbol{x};\varphi)$ is calculated in an anisotropic neighborhood to focus on fluctuations that are oriented in the azimuthal direction of the illumination. To this aim, a window function with a larger extent in the direction of the illumination is used.

This procedure ensures that only suitable groove structures account for the variance measure. Figure 7 explains the procedure with two images of a series: Firstly, the anisotropic smoothing suppresses intensity fluctuations which are oriented perpendicularly to the azimuth of the illumination, see Figs. 7(b) and (e). Due to the small extent of the smoothing function in the direction of the illumination, the contrast of ideally illuminated striae remains visible. Secondly, the measure of the local variance (Figs. 7(c) and (f)) shows maxima at positions, where the structures are oriented perpendicularly to the illumination azimuth.

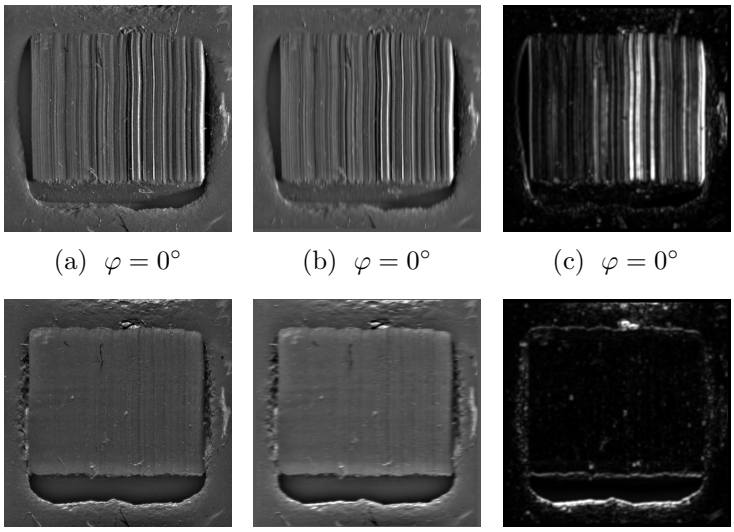

(a) $\varphi = 0°$ (b) $\varphi = 0°$ (c) $\varphi = 0°$

(d) $\varphi = 90°$ (e) $\varphi = 90°$ (f) $\varphi = 90°$

Figure 7. Computation of the local variance $\mathrm{var}(\boldsymbol{x};\varphi)$ with azimuth angles $\varphi = 0°$ and $\varphi = 90°$ of the illumination: (a), (d) unprocessed images; (b), (e) smoothed images; (c), (f) local variance.

3.2. Harmonic analysis

By interpreting the local variance $\mathrm{var}(\boldsymbol{x};\varphi)$ as a function of φ, an evaluation of its harmonic components can be performed for each location $\boldsymbol{x}$. Figure 8 depicts some typical curves for the intact striation pattern (left column) and the background (right column). At locations belonging to the striae, two distinct maxima with $\Delta\varphi = 180°$ can be found. Hence, the second harmonic of the local variance is emphasized. Its corresponding phase depends on the local groove direction $\vartheta(\boldsymbol{x})$. For locations in the background texture, maxima occur at varying azimuth angles φ, depending on the surface structure. Moreover, the second harmonic is less distinctive and without predominant phase.

The second harmonic is calculated using the Fourier Transform[10] of the local variance $\mathrm{var}(\boldsymbol{x};\varphi)$. An illumination series with K images is used, which has been acquired with azimuth angles equidistantly distributed over 360°. The Discrete Fourier Transform with respect to φ is then obtained by

$$S(\boldsymbol{x};n_\varphi) = \mathcal{F}\{\mathrm{var}(\boldsymbol{x}_\mathrm{p};\varphi)\} = \sum_{k=0}^{K-1} \mathrm{var}(\boldsymbol{x};\varphi_k)\ \exp\left(-\mathrm{j}\,2\pi\frac{kn_\varphi}{K}\right)\ . \tag{2}$$

To assign a location $\boldsymbol{x}$ to the groove area $\mathcal{T}$, two criteria must be met, which are then combined by a logical intersection:

- For the first condition, the local groove angle $\vartheta(\boldsymbol{x})$ is estimated with the phase of the second harmonic component $\angle\{S(\boldsymbol{x};n_\varphi = 2)\}$. The deviation of the estimation $\hat{\vartheta}(\boldsymbol{x})$ from an average groove angle $\overline{\vartheta}$ is imposed as the first feature. The criterion $\mathcal{T}_1$ for the groove area is then obtained with a circular threshold.

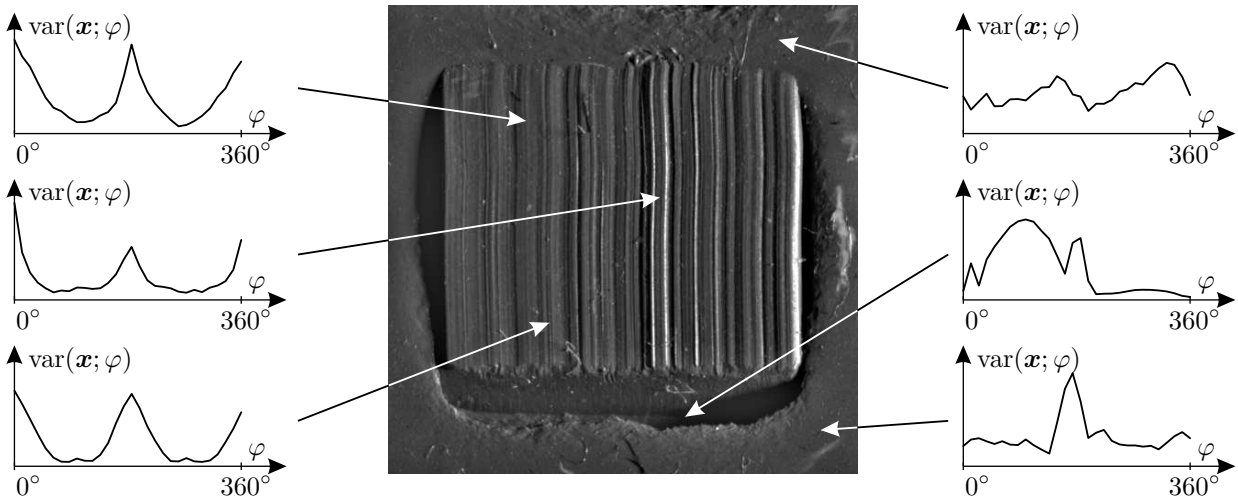

Figure 8. Typical curves for the local variance $\mathrm{var}(\boldsymbol{x};\varphi)$ for locations belonging to the striation pattern (left column) and to the background (right column).

Locations $\boldsymbol{x}$, where the estimated local groove angle differs from the average groove angle less than this threshold, are considered to meet the criterion $\mathcal{T}_1$.

- The second condition assesses the predominance of the second harmonic component in Fourier Space $S(\boldsymbol{x};n_\varphi)$ using the absolute value of the second harmonic component $|S(\boldsymbol{x};n_\varphi=2)|$. The criterion $\mathcal{T}_2$ for the groove area is then formulated using a second threshold which assesses the relative portion of the second harmonic compared to all harmonic components.

To show the performance of the presented strategy, Figs. 9(a)–(e) and 10(a)–(e) depict intermediate results at different stages obtained with the tool marks of Fig. 3. The assignment of each image location to the groove area or to the background area is coded in white or black, respectively. Although the exclusive application of a single criterion does not lead to sensible segmentation results, combination of both criteria $\mathcal{T}_1$ and $\mathcal{T}_2$ yields an acceptable preliminary classification of the groove area.

4. POSTPROCESSING

At this point, a binary mask is available that assigns each location either to the groove area or the background. However, this mask itself is not yet suitable for segmentation, since it still contains points which have been erroneously classified to belong to the groove area. Such misclassifications occur in small background areas that do not comply with the postulation of an isotropic background texture. Analogously, misclassifications, which are caused e. g. by dust particles and their shadows, are found in the striations. In consequence, a postprocessing has to be done to eliminate such errors.

The exactness of the masks can be improved significantly, if the relation of neighboring locations are taken into consideration. It is certainly more plausible that an image point belongs to the groove area, when all adjacent points are as well part of the groove area, than when only this point shows striation features. The postprocessing is composed of two steps:

- Firstly, small regions in the initially classified striation and background areas are removed by means of a morphological area opening and closing.[2,11,12] Figures 9(f) and 10(f) show the result of this processing.

- To improve the compactness of the striation area, the result of the preceding step is processed with a combination of morphological closing and opening.[12] To this aim, an elliptic structuring element, which is rotated so that it has its smaller extent in the direction of the average groove angle $\overline{\vartheta}$, is used. The

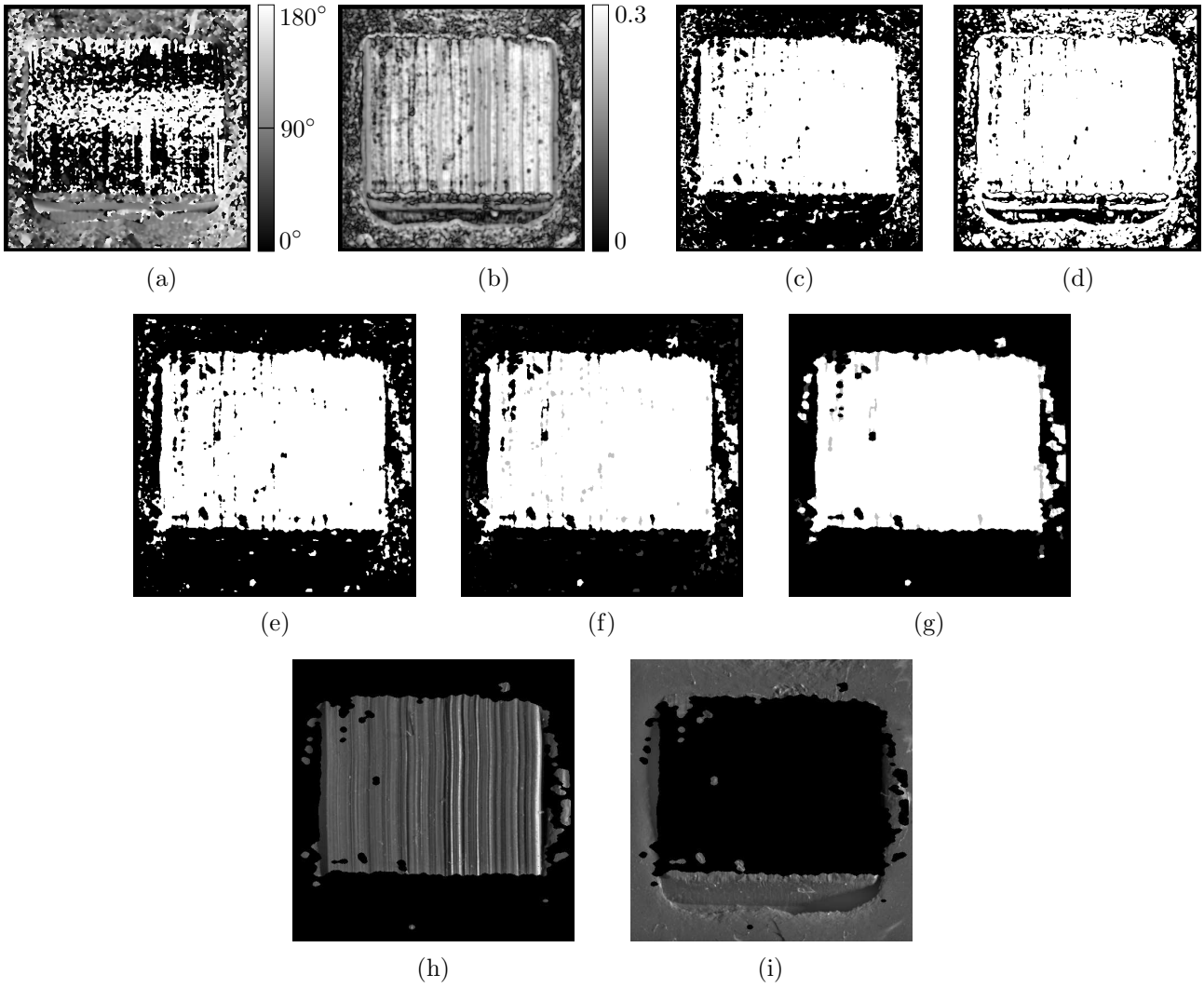

Figure 9. Segmentation results for Fig. 3(a): (a) estimation $\hat{\vartheta}(\boldsymbol{x})$ of the local groove angle;[†] (b) standardized absolute value of the second harmonic $|S(\boldsymbol{x}; n_\varphi = 2)|$; (c) criterion $\mathcal{T}_1$; (d) criterion $\mathcal{T}_2$; (e) fused criteria $\mathcal{T} = \mathcal{T}_1 \cap \mathcal{T}_2$; (f) result after morphological area opening and closing; (g) final segmentation mask after morphological closing and opening. Image points that have been added or removed are labelled in light and dark gray, resp.; (h) striation area; (i) background area.

anisotropic shape of the structuring element stimulates contiguous structures which are oriented perpendicularly to the direction of the striations. That way, the correct classification of areas with faint grooves is improved. Figures 9(g) and 10(g) show the resulting masks.

The segmented striation and background areas are shown in Figs. 9(h), (i) and 10(h), (i). Especially for the marks in Fig. 9, a good separation of the grooves and the background has been obtained. Real gaps in these marks are classified correctly. Outside of the striation area, some smaller regions are misclassified as grooves, however, these regions also have a groove-like texture.

5. CONCLUSIONS

In this contribution, a technique for the segmentation of striation patterns has been presented. It is based on an image series, in which the azimuth of a spot illumination is varied systematically. The basic idea is that the local

[†]The local groove angle is defined by the angle between the horizontal axis and the perpendicular to the grooves.

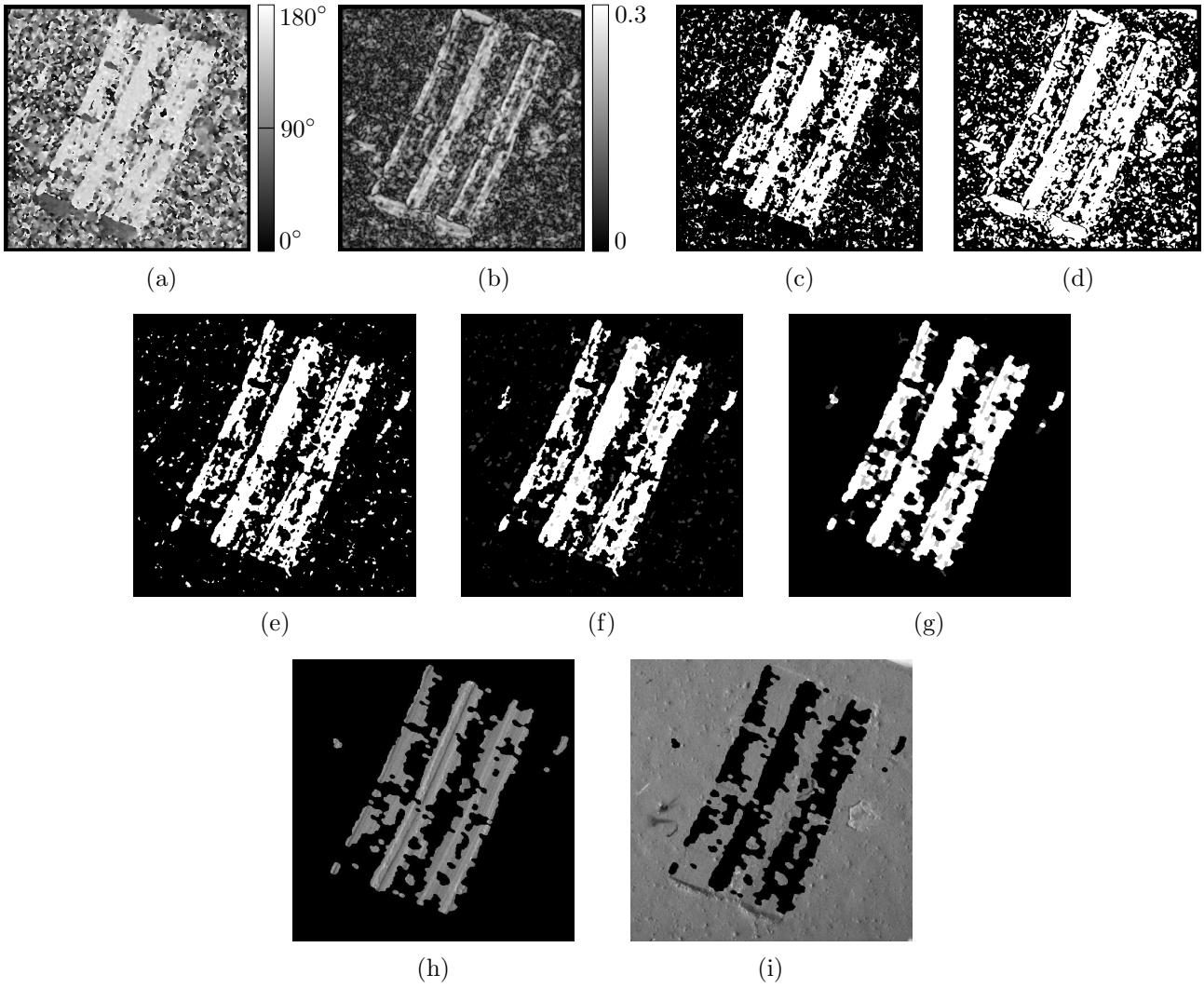

Figure 10. Segmentation results for Fig. 3(b): (a) estimation $\hat{\vartheta}(\boldsymbol{x})$ of the local groove angle; (b) standardized absolute value of the second harmonic $|S(\boldsymbol{x}; n_\varphi = 2)|$; (c) criterion $\mathcal{T}_1$; (d) criterion $\mathcal{T}_2$; (e) fused criteria $\mathcal{T} = \mathcal{T}_1 \cap \mathcal{T}_2$; (f) result after morphological area opening and closing; (g) final segmentation mask after morphological closing and opening. Image points that have been added or removed are labelled in light and dark gray, resp.; (h) striation area; (i) background area.

contrast changes with the illumination direction: It takes minima when the illumination comes from directions parallel to the grooves, whereas maxima are observed when the illumination is oriented perpendicularly. These local features are evaluated by means of a spectral analysis in the parameter domain of the illumination azimuth. The resulting preliminary mask is then improved in a two-stage morphological process in order to remove small misclassified regions. As a result, a segmentation mask is obtained, in which the interesting groove section of the mark is separated. That way, subsequent evaluation and comparison strategies can be optimized for the actual striation marks, thus leading to faster comparison algorithms and improved recognition results.

ACKNOWLEDGMENTS

The author would like to thank Dr. Horst Katterwe and his staff at BKA for their generous support of the work presented in this contribution.

REFERENCES

1. M. Heizmann and F. Puente León, "Automated analysis and comparison of striated toolmarks," in *Proceedings of the Fourth European Meeting for Shoeprint/Toolmark Examiners (SPTM 2001)*, H. Katterwe and A. Körschgen, eds., pp. 121–132, BKA, Wiesbaden, 2001.
2. M. Heizmann, *Auswertung von forensischen Riefenspuren mittels automatischer Sichtprüfung.* Phd thesis, Universität Karlsruhe (TH), Karlsruhe, 2004.
3. M. Heizmann, "Automated comparison of striation marks with the system GE/2," in *Investigative Image Processing II*, Z. J. Geradts and L. I. Rudin, eds., **4709**, pp. 80–91, SPIE, 2002.
4. C. Brein, "Model-based Segmentation of Impression Marks," in *Proceedings of the Fifth Meeting of the ENFSI Working Group Marks (SPTM 2005)*, Stavern, 2005.
5. M. Heizmann and F. Puente León, "Model-based analysis of striation patterns in forensic science," in *Enabling Technologies for Law Enforcement and Security*, S. K. Bramble, E. M. Carapezza, and L. I. Rudin, eds., **4232**, pp. 533–544, SPIE, 2001.
6. M. Heizmann and F. Puente León, "Imaging and analysis of forensic striation marks," *Optical Engineering* **42**(12), pp. 3423–3432, 2003.
7. F. Puente León, *Automatische Identifikation von Schußwaffen.* Phd thesis, Universität Karlsruhe (TH), Düsseldorf, 1999.
8. F. Puente León and M. Heizmann, "Strategies to detect non-linear similarities by means of correlation methods," in *Intelligent Robots and Computer Vision XX: Algorithms, Techniques, and Active Vision*, D. P. Casasent and E. L. Hall, eds., **4572**, pp. 513–524, SPIE, 2001.
9. M. Heizmann, "Segmentation of striation patterns using illumination series," in *Photonics in Measurement*, T. Pfeifer and R. Tutsch, eds., *VDI-Berichte* **1844**, pp. 461–470, VDI, 2004.
10. E. O. Brigham, *The fast Fourier transform and its applications*, Prentice-Hall, Englewood Cliffs, 1988.
11. J. Serra, *Image Analysis and Mathematical Morphology*, Academic Press, London, 1982.
12. P. Soille, *Morphological image analysis*, Springer-Verlag, Berlin, 1999.